

Searches for New Physics in Heavy Flavor Decays at CDF

R.F. Harr for the CDF Collaboration

Wayne State University
 Detroit, MI 48202 USA

Abstract

We present the most recent CDF heavy flavor results with sensitivity to physics beyond the standard model. These results include the search for and measurements of rare decays of B hadrons, and the measurement of CP violating asymmetries of charm and B hadrons. A number of the results represent the world's best measurements at this time, while others are among the world's best.

Keywords: CP Violation, Rare Decays, Bottom, Charm

1. Introduction

The CDF experiment has a long history of measurements of heavy flavor decays, pioneering many of the techniques for hadron collider experiments. With the termination of Tevatron operations, we are now producing final results of the most prominent analyses using the full dataset. The analyses discussed here deal with searches for rare decays and precision CP measurements that are sensitive to signs of new physics. Thus far these indirect searches do not yield a clear signal for new physics, and any new physics models must adhere to these constraints.

Information on the latest CDF results is available from the public results page [1]. The citations provided are primarily to the experimental results; citations to relevant theoretical works can be found in the cited experimental articles.

2. CP Violation in $B_s^0 \rightarrow J/\psi\phi$

The decay $B^0 \rightarrow J/\psi K_s^0$ is the golden mode for determining the CKM angle β . The analogous decay for the B_s^0 meson is $B_s^0 \rightarrow J/\psi\phi$ and it can be used to measure the corresponding angle β_s . While β is sizable, β_s is small in the standard model. The CP asymmetry $B_s^0 \rightarrow J/\psi\phi$ is poorly constrained, leaving room for the

presence of new particle couplings in $B_s^0-\bar{B}_s^0$ mixing to produce a measurable effect.

Table 1: The results of the $B_s^0 \rightarrow J/\psi\phi$ fit assuming the standard model value for β_s . The first error is statistical and the second systematic.

τ_s	$(1.528 \pm 0.019 \pm 0.009) \text{ ps}$
$\Delta\Gamma_s$	$(0.068 \pm 0.026 \pm 0.009) \text{ ps}^{-1}$
$ A_0 ^2$	$0.512 \pm 0.012 \pm 0.018$
$ A_{ } ^2$	$0.229 \pm 0.010 \pm 0.014$
δ_{\perp}	$2.79 \pm 0.53 \pm 0.15$

A result was previously published by CDF based on 5 fb^{-1} of integrated luminosity [2]. The updated analysis uses the full Run II dataset, about 9.6 fb^{-1} [3]. The selection and basic analysis techniques are adapted from the previous analysis. The fit to extract the CP violating phase includes angular variables, lifetime, mass, and tagging information. Opposite-side tagging is validated for and used on the full dataset; same-side kaon tagging is used on the first 5.2 fb^{-1} of integrated luminosity where it had been validated for the previous analysis. The results of the fit assuming the standard model value for β_s are displayed in Table 1. The results of the fit

for $\phi_s = -2\beta_s$ versus $\Delta\Gamma_s$ are shown in Fig. 1, including full coverage adjustment. The results are consistent with the standard model and the results from D0, LHCb, and ATLAS [4, 5, 6].

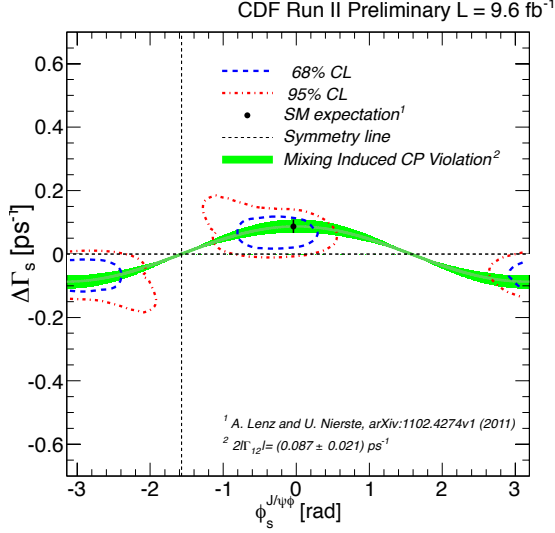


Figure 1: The $1\text{-}\sigma$ and $2\text{-}\sigma$ contours for ϕ_s versus $\Delta\Gamma_s$ are indicated by the dashed (blue) and dot-dashed (red) curves, including coverage adjustment. The solution is symmetric under a simultaneous transformation $\phi_s \rightarrow \pi/2 - \phi_s$ and $\Delta\Gamma_s \rightarrow -\Delta\Gamma_s$ indicated by the dotted (black) lines. The standard model prediction is indicated by the dot with error bar, and the green region is consistent with all the CP violation originating in mixing.

Aside from the addition of more data, the main improvement in this analysis is a more detailed study of the components of the K^+K^- mass distribution in the $B_s^0 \rightarrow J/\psi K^+K^-$ final state. The D0 experiment found a rather large S -wave contribution [4] which could have a significant impact on the CDF analysis. To measure the contributions, the K^+K^- mass range is widened to $m_{KK} \in [0.988, 1.200] \text{ GeV}/c^2$ and a simultaneous fit to the $J/\psi K^+K^-$ and K^+K^- mass distributions is performed. The K^+K^- mass fit includes a relativistic Breit-Wigner for the ϕ , a Flatté function for the $f_0(980)$, background from misidentified $B^0 \rightarrow J/\psi K^+\pi^-$ decays, and a background distribution derived from the data. The S -wave contribution in the K^+K^- mass range used for $B_s^0 \rightarrow J/\psi\phi$ events is $(0.8 \pm 0.2(\text{stat}))\%$, consistent with results from LHCb and ATLAS [5, 6]. The misidentified $B^0 \rightarrow J/\psi K^+\pi^-$ is determined to be $(8.0 \pm 0.2(\text{stat}))\%$. This is a larger value than most experiments determine and could explain the large S -wave component found in the D0 analysis.

3. Search for $B_{(s)}^0 \rightarrow \mu^+\mu^-$

The decay $B_s^0 \rightarrow \mu^+\mu^-$ is very sensitive to the presence of new physics, and supersymmetry in particular. It has been the subject of 4 previous searches by CDF. The previous search [10] using 7 fb^{-1} of integrated luminosity indicated a small excess of events in the B_s^0 mass window but no excess in the B^0 mass window. This latest result uses the full Run II dataset, corresponding to about 9.6 fb^{-1} of integrated luminosity [11]. The same neural network as used in the 7 fb^{-1} analysis is used in the update, without retraining. This has the advantage of allowing a quick processing of the additional data with no bias introduced.

The results of the analysis are displayed in Figs. 2 for the B^0 mass window. There is no evidence for an excess of events in the $B^0 \rightarrow \mu^+\mu^-$ mass window, and we set a limit on the decay of

$$\mathcal{B}(B^0 \rightarrow \mu^+\mu^-) < 4.6 \text{ (3.8)} \times 10^{-9} \quad (1)$$

at the 95% (90%) confidence level.

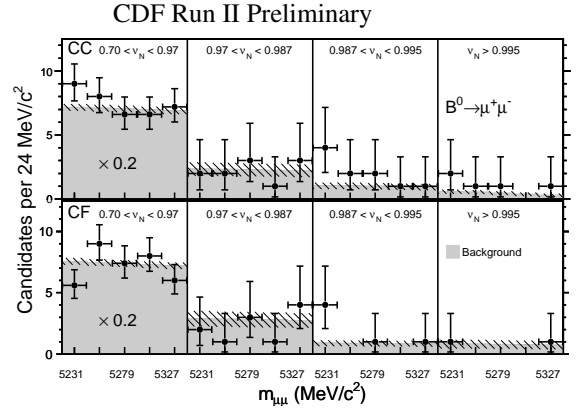


Figure 2: The dimuon mass distribution for the B^0 mass window. The events are divided into those with two muons in the central muon detector (CC) and those with a central and a forward muon (CF). The events are further divided by NN score, where a score near 1 is more signal-like. No excess is seen in these results.

The results for the B_s^0 mass window are displayed in Fig. 3. These data show a mild excess with a p-value for the background-only hypothesis of 0.94%, and a p-value for background plus standard model signal of 7.1%. Using a log-likelihood technique, we find the best fit value for the branching fraction and 1σ errors to be

$$\mathcal{B}(B_s^0 \rightarrow \mu^+\mu^-) = (1.3_{-0.7}^{+0.9}) \times 10^{-8}. \quad (2)$$

Using a CLs technique we determine two-sided limits for the branching ratio of

$$0.8 \text{ (2.2)} \times 10^{-9} < \mathcal{B}(B_s^0 \rightarrow \mu^+\mu^-) < 34 \text{ (30)} \times 10^{-9} \quad (3)$$

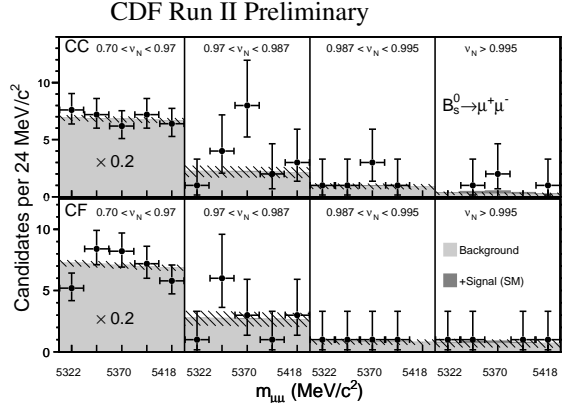


Figure 3: The dimuon mass distribution for the B_s^0 mass window. The events are divided into those with two muons in the central muon detector (CC) and those with a central and a forward muon (CF). The events are further divided by NN score, where a score near 1 is more signal-like. There is a small excess in the two most signal-like CC mass plots.

at the 95% (90%) confidence level. This result is consistent with, and an improvement over our previous result. The p-values are higher for both background-only and signal plus background assumptions. It is consistent with the standard model prediction and with the results from D0, ATLAS, CMS and LHCb as shown in Fig. 4.

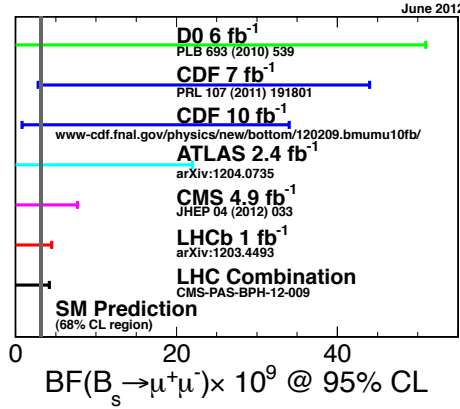


Figure 4: The recent results for searches for $B_s^0 \rightarrow \mu^+ \mu^-$ and the standard model prediction.

4. Measurements of $b \rightarrow s\mu^+\mu^-$ Decays

Flavor-changing neutral-current decays of the type $b \rightarrow s\mu^+\mu^-$ are strongly suppressed and another promis-

ing place to search for signs of new physics. Decays of this type include $B^0 \rightarrow K^{*0}\mu^+\mu^-$, $B^0 \rightarrow K_S^0\mu^+\mu^-$, $B^+ \rightarrow K^{*+}\mu^+\mu^-$, $B^+ \rightarrow K^+\mu^+\mu^-$, $B_s^0 \rightarrow \phi\mu^+\mu^-$, and $\Lambda_b \rightarrow \Lambda\mu^+\mu^-$. These last two modes were first observed by CDF in a previous analysis [7].

The update uses the full Run II dataset and optimizes the signal yields for all of the modes listed above [8]. The yields in each mode are measured relative to the corresponding mode where the $\mu^+\mu^-$ pair comes from a $J/\psi \rightarrow \mu^+\mu^-$ decay. The resulting branching ratios are reported in Table 2. We also measure the differential branching ratio as a function of the square of the $\mu^+\mu^-$ invariant mass, q^2 . These results are available in the more detailed write-up [8].

Table 2: Branching fractions for the $b \rightarrow s\mu^+\mu^-$ flavor-changing neutral-current decay modes. The first error is statistical and the second is systematic.

Mode	Branching Fraction $\times 10^6$
$B^+ \rightarrow K^+\mu^+\mu^-$	$0.45 \pm 0.03 \pm 0.02$
$B^0 \rightarrow K^{*0}\mu^+\mu^-$	$1.14 \pm 0.09 \pm 0.06$
$B_s^0 \rightarrow \phi\mu^+\mu^-$	$1.17 \pm 0.18 \pm 0.37$
$B^0 \rightarrow K^0\mu^+\mu^-$	$0.33 \pm 0.08 \pm 0.03$
$B^+ \rightarrow K^{*+}\mu^+\mu^-$	$0.89 \pm 0.25 \pm 0.09$
$\Lambda_b^0 \rightarrow \Lambda\mu^+\mu^-$	$1.95 \pm 0.34 \pm 0.61$

Additional sensitivity is obtained by combining the measurements for the neutral and charged K and K^* modes. They are combined assuming isospin symmetry, so we first check the validity of that assumption, reporting the isospin asymmetry between the neutral and charged modes as a function of q^2 , in Fig. 5. There is no evidence for violation of isospin symmetry in either the K or K^* modes.

There are a number of angular observables that can be probed and provide additional sensitivity to new physics. We choose to look at the forward-backward asymmetry of muons, A_{FB} ; longitudinal polarization fraction of the K^* , F_L ; transverse polarization asymmetry, $A_T^{(2)}$; and triple product asymmetry, A_{im} . We measure these for the flavor specific K and K^* modes — limited sample size precludes a meaningful measurement for the Λ_b mode. Figure 6 displays the results versus q^2 for the K^* modes combined assuming isospin symmetry. The red curves show the predictions from the standard model [9]. The measurements show no indications of new physics at this level of accuracy.

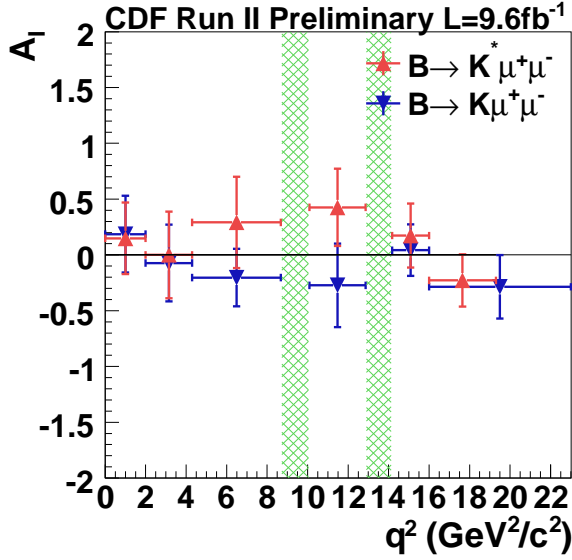


Figure 5: Isospin asymmetry versus q^2 between decays involving charged and neutral K^* mesons (red) and charged and neutral K mesons (blue). The green shaded bands indicate excluded mass ranges around the J/ψ and ψ' resonances.

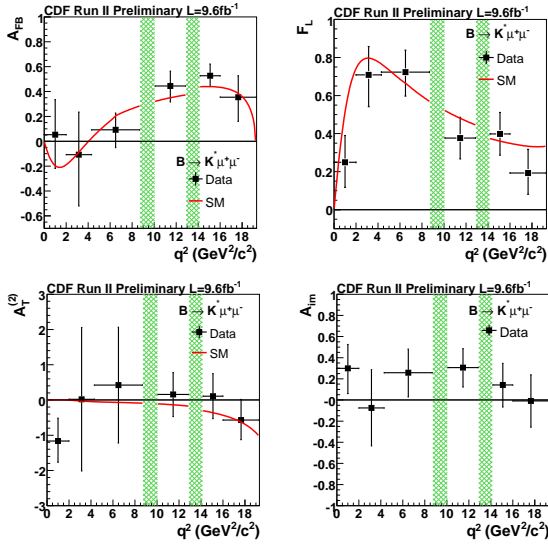


Figure 6: The forward-backward asymmetry of muons, A_{FB} (upper left), longitudinal polarization fraction of the K^* , F_L (upper right), transverse polarization asymmetry, $A_T^{(2)}$ (lower left), and triple product asymmetry, A_{im} (lower right) for the combined $B \rightarrow K^* \mu^+ \mu^-$ data as a function of square of the invariant mass of the muons, q^2 . The green shaded bands indicate the excluded mass ranges around the J/ψ and ψ' resonances.

5. CP Asymmetries in $H_b \rightarrow h^+ h'^-$ Decays

Charmless decays of B hadrons are strongly suppressed, with sizable penguin amplitudes. New physics can appear in the decay and interfere with standard model decay paths to produce sizable asymmetries. It has been suggested [12, 13] that the $B_s^0 \rightarrow K^- \pi^+$ asymmetry can be used in a model independent test to resolve the puzzling difference between CP violating asymmetries in charged and neutral $B \rightarrow K\pi$ decays. And asymmetries in charmless Λ_b decays have never been explored and could contribute additional insight.

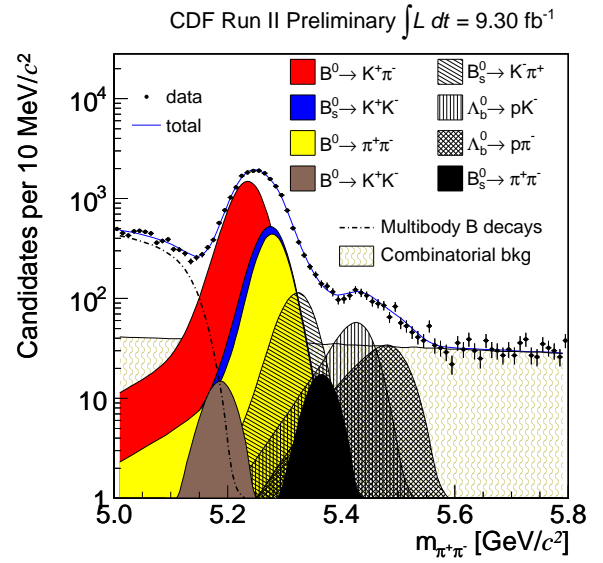


Figure 7: The distribution of invariant mass for the two-track candidates, treating both tracks as pions. The shaded contours indicate the components of the fit to the data. Note the logarithmic scale used to enhance the visibility of the smaller components.

The displaced vertex trigger [14] of CDF is effective at selecting two-body B hadron decays, as indicated by the data and fit results shown in Fig. 7. The data are selected with the same procedure used in an earlier analysis [15]. The updated analysis uses all of the data from Run II of the Tevatron, corresponding to about 9.3 fb^{-1} of integrated luminosity. The fits to the data is complex and includes 8 decay components, radiative tails, mass mis-assignment effects, and backgrounds. The fit makes use of information in addition to $m_{\pi\pi}$ to separate the decay components: the scalar sum of the daughter momenta, the momentum asymmetry, the difference in kaon hypothesis variables derived from track dE/dx , and the sum of the same variables. Each of these adds sensitivity to help separate the fit components for the final result.

Table 3: The asymmetries in charmless 2-body B hadron decays. The first error is statistical and the second systematic.

mode	A_{CP}
$B^0 \rightarrow K^+\pi^-$	$-0.083 \pm 0.013 \pm 0.003$
$B_s^0 \rightarrow K^-\pi^+$	$0.22 \pm 0.07 \pm 0.02$
$\Lambda_b^0 \rightarrow p\pi^-$	$0.07 \pm 0.07 \pm 0.03$
$\Lambda_b^0 \rightarrow pK^-$	$-0.09 \pm 0.08 \pm 0.04$

The asymmetry results are listed in Table 3. The nonzero asymmetry of the $B^0 \rightarrow K^+\pi^-$ decay is well established [17]. The $B_s^0 \rightarrow K^-\pi^+$ asymmetry is 3σ from zero, confirming and consistent with the evidence reported by the LHCb collaboration [18]. The asymmetries measured for the Λ_b decays are consistent with zero at the present level of precision.

6. $D^0 \rightarrow K^+K^-$ and $D^0 \rightarrow \pi^+\pi^-$ CP Asymmetries

One of the most interesting new avenues in the search for new physics is CP violation in charm decays. The first evidence for CP violation in charm decays emerged from the LHCb experiment [19] in the difference of CP asymmetries between $D^0 \rightarrow K^+K^-$ and $D^0 \rightarrow \pi^+\pi^-$. After the LHCb result, it was realized that the standard model prediction is difficult to determine accurately and could be of the order of 1% in some channels, consistent with the evidence. However, in the standard model the two modes are expected to have CP asymmetries of opposite sign, enhancing the sensitivity of the difference.

The CDF experiment had produced the most precise measurement to date of the CP asymmetries of $D^0 \rightarrow \pi^+\pi^-$ and $D^0 \rightarrow K^+K^-$ [20] shortly before the LHCb result. The result for the individual asymmetries was consistent with the LHCb result, but it was realized that the difference could be measured more precisely by optimizing the selection to measure the asymmetry difference [21]. The CP asymmetry is defined as

$$A_{CP}(D^0 \rightarrow h^+h^-) = \frac{\Gamma(D^0 \rightarrow h^+h^-) - \Gamma(\bar{D}^0 \rightarrow h^+h^-)}{\Gamma(D^0 \rightarrow h^+h^-) + \Gamma(\bar{D}^0 \rightarrow h^+h^-)} \quad (4)$$

where h is either K or π . The asymmetry difference to be measured is

$$\Delta A_{CP} = A_{CP}(D^0 \rightarrow K^+K^-) - A_{CP}(D^0 \rightarrow \pi^+\pi^-). \quad (5)$$

The flavor of the D^0 is determined by using D^{*+} from D^{*+} decays, and the charge conjugate decays. The sign of the pion from the strong decay of the D^* determines the flavor; D^{*+} decay to D^0 and D^{*-} decay to \bar{D}^0 .

The energy available in the D^* decay is small resulting in low transverse momentum pions from the decay. The CDF tracking detector has an efficiency asymmetry for low p_T tracks of opposite charge. This detector induced asymmetry is effectively cancelled in Eq. 5. Other non- D^0 asymmetries are also cancelled in the difference of asymmetries, including a possible asymmetry of D^0 's originating from an asymmetry in the decays of B hadrons. The asymmetry difference is calculated from the numbers of D^{*+} 's determined in the fits to the data displayed in Fig. 8. The result using the full Run II data set is

$$\Delta A_{CP} = (-0.62 \pm 0.21 \pm 0.10) \% \quad (6)$$

where the first error is statistical and the second systematic. This result is 2.7σ different from zero and consistent with the LHCb evidence. The combination of this result with the LHCb result is 3.8σ from zero.

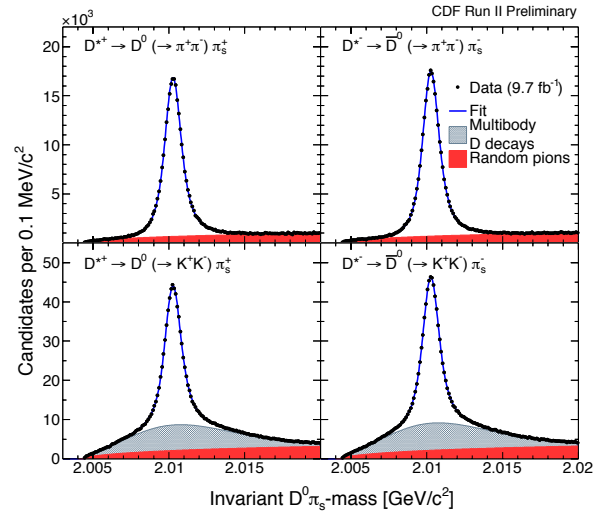


Figure 8: The D^{*+} candidate mass distributions for $D^0\pi^+$ (left column) and $\bar{D}^0\pi^+$ (right column). The events where the D^0 or \bar{D}^0 candidate decays to $\pi^+\pi^-$ are displayed in the top row, while those to K^+K^- are in the bottom row.

The result is a combination of direct CP violation, having no time dependence, and indirect CP violation with time dependence. The time integrated CP asymmetry arises from a combination of these according to the expression

$$\Delta A_{CP} = \Delta A_{CP}^{\text{dir}} + \frac{\Delta\langle t \rangle}{\tau} A_{CP}^{\text{ind}} \quad (7)$$

where $\Delta A_{CP}^{\text{dir}}$ is the difference of direct CP asymmetries between the KK and $\pi\pi$ modes, A_{CP}^{ind} is the indirect CP asymmetry assumed to be independent of the

mode, $\Delta\langle t \rangle$ is the difference in average decay times for the events in the two modes, and τ is the D^0 lifetime. All available results have been compiled by the Heavy Flavor Averaging Group and are displayed in Fig. 6. The global combination is about 4σ from the zero CP violation point.

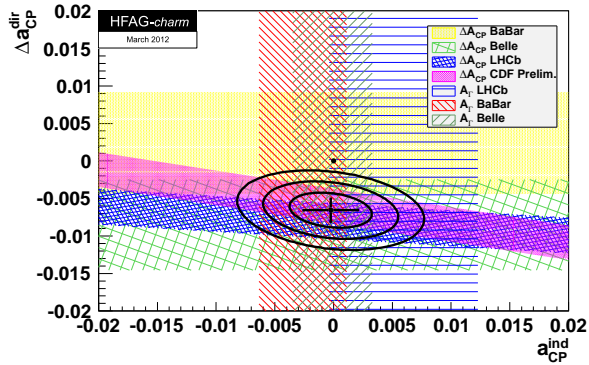


Figure 9: The compilation of charm A_{CP} differences by the Heavy Flavor Averaging Group. Figure taken from <http://www.slac.stanford.edu/xorg/hfag/charm/index.html>.

7. Summary

The CDF experiment has updated many of the flagship analyses using the full Run II dataset. The analyses discussed here are those with sensitivity to the effects of new physics: searches for rare decays, and CP asymmetry measurements in heavy flavor decays. Most of the results are consistent with standard model predictions at the present level of accuracy. The measurement of the CP asymmetry difference between $D^0 \rightarrow K^+ K^-$ and $D^0 \rightarrow \pi^+ \pi^-$ is the outstanding exception, however the standard model prediction is rather difficult to make. More data on other charm decays could help to constrain the theory and provide a more definitive answer to whether the measurement is consistent with the standard model.

References

- [1] CDF B Group Public Results Page, <http://www-cdf.fnal.gov/physics/new/bottom/bottom.html>.
- [2] T. Aaltonen *et al.* (CDF Collaboration), Phys. Rev. D **85**, 072002 (2012).
- [3] T. Aaltonen *et al.* (CDF Collaboration), arXiv:1208.2967 (2012), submitted to PRL.
- [4] V.M. Abazov *et al.* (D0 Collaboration), Phys. Rev. D **85**, 032006 (2012).
- [5] R. Aaij *et al.* (LHCb Collaboration), Phys. Rev. Lett. **108**, 101803 (2012).
- [6] G. Aad *et al.* (ATLAS Collaboration), arXiv:1208.0572 (2012).
- [7] T. Aaltonen *et al.* (CDF Collaboration), Phys. Rev. Lett. **107**, 201802 (2011).
- [8] CDF Collaboration, CDF Public Note 10894 (2012).
- [9] Y.-M. Wang, M.J. Aslam, and C.-D. Lu, Eur. Phys. J. C **59**, 847 (2009); P. Ball and R. Zwicky, Phys. Rev. D **71**, 014015 (2005); P. Ball and R. Zwicky, Phys. Rev. D **71**, 014029 (2005); T.M. Aliev, K. Azizi, and M. Savci, Phys. Rev. D **81**, 056006 (2010).
- [10] T. Aaltonen *et al.* (CDF Collaboration), Phys. Rev. Lett. **107**, 191801 (2011).
- [11] M. Dorigo for the CDF Collaboration, arXiv:1205.3899 (2012).
- [12] M. Gronau and J.L. Rosner, Phys. Lett. B **482**, 71 (2000).
- [13] H.J. Lipkin, Phys. Lett. B **621**, 126 (2005).
- [14] L. Ristori and G. Punzi, Ann. Rev. Nucl. Part. Sci. **60**, 595 (2010).
- [15] T. Aaltonen *et al.* (CDF Collaboration), Phys. Rev. Lett. **103**, 031801 (2009).
- [16] CDF Collaboration, CDF Public Note 10726 (2012).
- [17] J. Beringer *et al.* (Particle Data Group), Phys. Rev. D **86**, 010001 (2012).
- [18] R. Aaij *et al.* (LHCb Collaboration), Phys. Rev. Lett. **108**, 201601 (2012).
- [19] R. Aaij *et al.* (LHCb Collaboration), Phys. Rev. Lett. **108**, 111602 (2012).
- [20] T. Aaltonen *et al.* (CDF Collaboration), Phys. Rev. D **85**, 012009 (2012).
- [21] T. Aaltonen *et al.* (CDF Collaboration), Phys. Rev. Lett. **109**, 111801 (2012).